AIP Applied Physics Letters

Magnetic properties of Co2C and Co3C nanoparticles and their assemblies

Kyler J. Carroll, Zachary J. Huba, Steven R. Spurgeon, Meichun Qian, Shiv N. Khanna et al.

Citation: Appl. Phys. Lett. **101**, 012409 (2012); doi: 10.1063/1.4733321
View online: http://dx.doi.org/10.1063/1.4733321
View Table of Contents: http://apl.aip.org/resource/1/APPLAB/v101/i1
Published by the American Institute of Physics.

Related Articles

Dynamical mean-field theory for molecules and nanostructures
J. Chem. Phys. 136, 114108 (2012)

Size, surface structure, and doping effects on ferromagnetism in SnO2
J. Appl. Phys. 111, 07C321 (2012)

Half metallicity and electronic structures in armchair BCN-hybrid nanoribbons
J. Chem. Phys. 134, 074708 (2011)

Studies on structures, electronic and magnetic properties of TM-doped InnSbn (n = 7–12,14,16) clusters (TM = Mn, Fe, and Co)
J. Appl. Phys. 109, 014322 (2011)

Additional information on Appl. Phys. Lett.

Journal Homepage: http://apl.aip.org/
Journal Information: http://apl.aip.org/about/about_the_journal
Top downloads: http://apl.aip.org/features/most_downloaded
Information for Authors: http://apl.aip.org/authors

ADVERTISEMENT

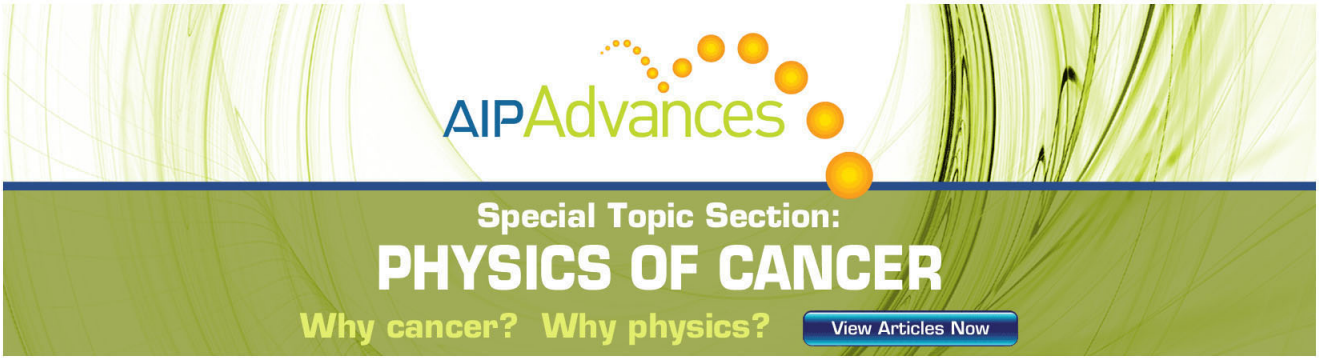

Downloaded 06 Jul 2012 to 129.25.131.235. Redistribution subject to AIP license or copyright; see http://apl.aip.org/about/rights_and_permissions

Magnetic properties of Co_2C and Co_3C nanoparticles and their assemblies

Kyler J. Carroll,[1,2,a)] Zachary J. Huba,[1,a)] Steven R. Spurgeon,[3] Meichun Qian,[4] Shiv N. Khanna,[4] Daniel M. Hudgins,[1] Mitra L. Taheri,[3] and Everett E. Carpenter[1,b)]
[1]*Department of Chemistry, Virginia Commonwealth University, Richmond, Virginia 23284, USA*
[2]*Department of NanoEngineering, University of California, San Diego, La Jolla, California 92093, USA*
[3]*Department of Materials Science and Engineering, Drexel University, Philadelphia, Pennsylvania 19104, USA*
[4]*Department of Physics, Virginia Commonwealth University, Richmond, Virginia 23284, USA*

(Received 21 May 2012; accepted 9 June 2012; published online 6 July 2012)

Nano-composite material consisting of Co_2C and Co_3C nanoparticles has recently been shown to exhibit unusually large coercivities and energy products. Experimental studies that can delineate the properties of individual phases have been undertaken and provide information on how the coercivities and the energy product change with the size and composition of the nanoparticles. The studies indicate that while both phases are magnetic, the Co_3C has higher magnetization and coercivity compared to Co_2C. Through first principles electronic structure studies using a GGA+U functional, we provide insight on the role of C intercalation on enhancing the magnetic anisotropy of the individual phases. © *2012 American Institute of Physics*. [http://dx.doi.org/10.1063/1.4733321]

Permanent magnets are an indispensable component in many applications such as hybrid electric vehicles, wind power, magnetic refrigeration, and flywheel energy storage. The key parameter controlling the performance is the magnetic energy density, typically presented via the maximum energy product $(BH)_{max}$, since it leads to an increase in the whole device efficiency (for example the volume-to-power ratio of an electric motor).[1–4] For single phase material, since the development of rare earth permanent magnets in the 1970s, there have been minor advances in the $(BH)_{max}$, achieved mainly by varying the synthetic processing and the ability to control the anisotropy. An alternate approach is to develop a multi-phase material consisting of an assembly of hard and soft phase nanoparticles that interact via exchange coupling. This approach is particularly exciting in view of the recent developments in chemical synthesis methods of nanoparticles that allow for size and composition control. These nanoparticles have atomic structures and compositions often different from the bulk stable phases. One can then tune the magnetic properties of the resulting material by controlling the magnetic characteristics of the mixed phase nanoparticles, serving as building blocks of the assembled material.

In a recent paper,[4] some of the present authors reported synthesizing a nanocomposite material composed of a mixture of Co_2C and Co_3C nanoparticles of varying size using polyol reduction chemistry. The material offered unusual magnetic properties with a maximum high energy product greater than 20 kJ m^{-3} and coercivity greater than 3.4 kOe and these properties changed with the size and ratio of the mixing nanoparticles. These are remarkable findings particularly since the composite nano-material did not contain any 5d transition or rare earth elements. It is interesting to note that bulk fcc Co is a soft magnetic material. The magnetic anisotropy increases in going to hcp phase or introducing stacking faults. These observations indicate that the coercivity can be controlled by changing the atomic spacing as well as the symmetry.[5,6] The unusually large observed coercivity in Co_2C and Co_3C nano-assemblies, probably arises due to further enhancements in anisotropy in the individual nanoparticles due to mixing between Co and C states, as well as due to cooperative effects in the assembled material.[7] A fundamental understanding of the effect of particle size, morphology, and composition on the magnetic properties of individual phases is critical to translate these initial findings into a nano-assembled material that has the potential to compete with rare earth magnets. The purpose of the present paper is to use a synergistic approach consisting of synthesizing well characterized carbide phase nanoparticles along with first principles investigations to provide insight into some of these basic issues. In particular, we characterize the atomic structure of each phase and demonstrate how the magnetic moment and the energy product of the nanocomposite material vary with size of the assembled nanoparticles. Through first principles calculations we then provide insight into how the incorporation of carbon (C) atoms into the metallic cobalt (Co) structure increases the anisotropy of individual phases, playing a similar role to samarium or neodymium in current rare earth permanent magnets.[2–4]

The synthesis of Co_xC nanoparticles is accomplished using a wet chemical technique, known as the polyol process.[4,8] In brief, the polyol process can be used to reduce metal salts by using a base deprotonated, polyhydric alcohol (polyol), allowing for a ligand exchange to occur between the deprotonated alcohol, or glycolate, and the metal salt ligand.[9] Excess glycolate ions then assist in the reduction of the metal at elevated temperatures and act as a capping agent. Therefore, by controlling the amount of base and reaction temperature, the reduction, nucleation, and growth dynamics can be intimately controlled. In this study, formation of cobalt carbide crystal phases show a strong dependence

[a)]Kyler J. Carroll and Zachary J. Huba contributed equally to this paper.
[b)]Author to whom correspondence should be addressed. Electronic mail: ecarpenter2@vcu.edu.

 © 2012 American Institute of Physics

Downloaded 06 Jul 2012 to 129.25.131.235. Redistribution subject to AIP license or copyright; see http://apl.aip.org/about/rights_and_permissions

on the hydroxide concentration [OH^-] when using a high boiling point polyol such as tetraethylene glycol (TEG, BP = 325 °C) (Figure 1(a)). Thus, by controlling the nucleation and growth rates through [OH^-] and temperature, the synthesis of pure phase Co_3C and Co_2C can be precisely controlled (Figure 1(b)). The addition of OH^- increases the amount of capping agent and lowers the distillation temperature of the solvent, slowing nucleation and growth (S1).[10,11] Slowing the growth rate is essential to forming the desired carbide phases, as we believe that cobalt carbide forms due to a surface reconstruction/diffusion of C atoms into the Co structure.[12–15] Therefore, the surface diffusion of C and particle growth are competing events. If growth is too rapid, complete diffusion of the C will not occur at the relatively low reaction temperatures, resulting in metallic Co impurities. By controlling growth dynamics through synthesis parameters, we have been able to synthesize highly coercive Co_xC particles as well as other transition metal carbides using various precursor salts and solvents. (S2).

The synthesis of bulk transition metal carbides is most commonly carried out by mixing metal and C powders and heating to temperatures in excess of 600 °C, while the wet chemical synthesis of Co_xC particles occurs at lower temperatures, less than 300 °C, making the technique more efficient and allowing for better phase control.[16,17] The reaction conditions for Co_xC particles are very similar to the reaction conditions used during the Fischer Tropsch (FT) synthesis, where the formation of cobalt carbide phases are also reported, however as a poisoning mechanism of the Co metal catalysts.[13,18–21] In FT catalysis, carbon monoxide and hydrogen gases are flowed over a transition metal catalyst, whereby the carbon monoxide is catalytically decomposed to C atoms which over time transform the catalyst to a carbide through a surface diffusion mechanism.[12,13] We propose that the cobalt carbide formation, by the polyol process, occurs similarly to carbides formed during the FT synthesis with the source of carbon monoxide being the aldehyde formed during the reduction of cobalt.[9,22] Preliminary results show Co to be an effective catalyst towards the decarbonylation of aldehydes. The proposed mechanism along with preliminary results can be found in the supporting information (S4).[41]

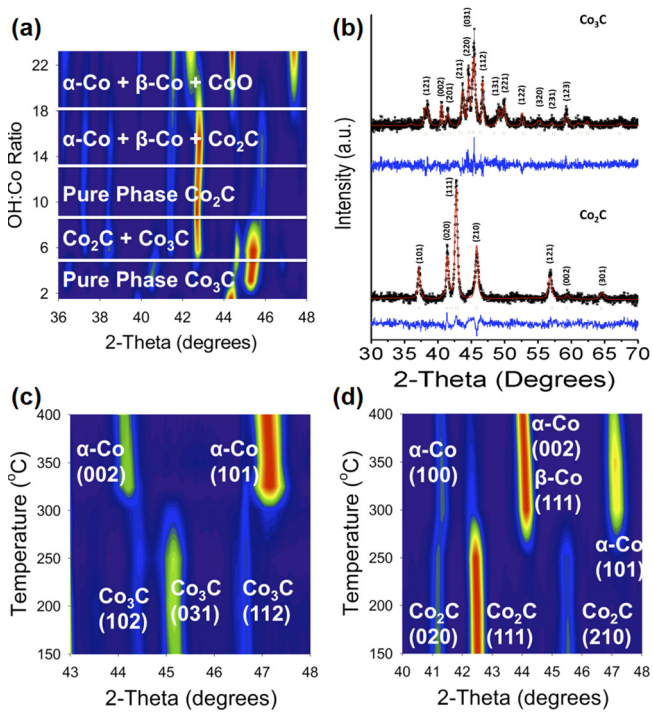

FIG. 1. (a) Contour plot showing the effect of OH:Co ratio on crystal phase formed. Co_3C was formed at a OH:Co ratio of 4:1, while Co_2C at ratios from 10:1–14:1. (b) Reitveld refinement of the x-ray diffraction patterns for as prepared Co_3C (top) and Co_2C (bottom). ETXRD scans of (c) Co_3C and (d) Co_2C show the decomposition of the carbide crystal phases into metallic cobalt phases.

When looking at the *3d* transition metals used as FT catalysts metallic Co is unique in that it has two stable low temperature allotropes, the α (hexagonal close packed) and β (face centered cubic) phases. In lower boiling point polyols, the synthesis of the α and (β-Co) phases can be controlled by changing the [OH^-].[23–26] At low [OH^-], the kinetic product (α-Co) is formed upon nucleation while higher concentrations form the thermodynamic product (β-Co).[23] Comparing the phase control seen in metallic Co nanoparticles with that of the phase control we present with the Co_xC nanoparticles, we believe that the initial nucleated Co species affects the resulting carbide phase. To investigate this, we used elevated temperature x-ray diffraction (ETXRD), which revealed Co_3C to decompose to α-Co while Co_2C transitioned to the α and β-Co phases at 325 °C and 275 °C, respectively (Figures 1(c) and 1(d)). The crystal structure of Co_3C is isomorphous to that of Fe_3C (cementite), which is commonly visualized as a twinning of HCP-Fe unit cells with C atoms filling interstitial sites.[27,28] The identification that Co_3C is synthesized at similar [OH^-] to α-Co (HCP) and decomposes into the α-Co (HCP) points to the nucleation of α-Co particles being essential to the formation of Co_3C. The formation of Co_2C is relatively more difficult to unravel, since it decomposes into both α- and β-Co phases. Comparing Co_2C to Ni_2C, the formation of Ni_2C is thermodynamically favorable above a minimum threshold of surface C coverage on the catalyst particle surface, hence the formation of Co_2C might be independent of nucleated particle structure.[14] The higher [OH^-] used in the synthesis of Co_2C slows growth allowing for more surface C atom coverage and directing the formation of Co_2C. Further investigations using *in-situ* synchrotron based x-ray techniques are scheduled and will help to shed more light on the formation mechanics of the Co_3C and Co_2C phases.

Synthesized Co_2C and Co_3C particles possess an average secondary particle diameter around 300 nm (Figures 2(a) and 2(d)). High-resolution TEM images of the particle surfaces reveal the presence of a glycolate layer and primary crystallites attached to the larger agglomerates (Figures 2(b) and 2(e)). This polycrystalline assembly was also confirmed from SAED and XRD analysis. Fourier transforms confirm lattice parameters of a = 5.05 Å and c = 4.48 Å for Co_3C (Figures 2(b) and 2(c)) and lattice parameters of a = 4.50 Å and c = 2.91 Å for Co_2C (Figures 2(e) and 2(f)), commensurate with the values obtained from x-ray diffraction. The glycolate layer on the surface was confirmed using x-ray photoelectron spectroscopy (XPS), however due to the

Downloaded 06 Jul 2012 to 129.25.131.235. Redistribution subject to AIP license or copyright; see http://apl.aip.org/about/rights_and_permissions

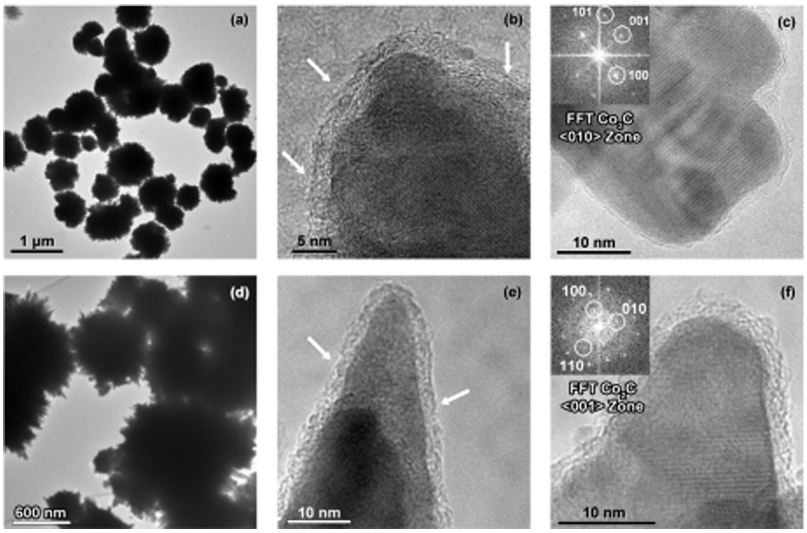

FIG. 2. Bright field TEM images of (a) Co_3C particles, (b) Co_3C particle surface showing the presence of a gylcolate layer and fine crystallites, indicated by arrows, (c) HRTEM of Co_3C particles showing glycolate layer and inset FFT corresponding to Co_3C ⟨010⟩ zone axis, (d) Co_2C particles, (e) Co_2C particles showing the glycolate later, and (f) HRTEM of Co_2C particles showing the glycolate layer and inset FFT corresponding to Co_2C ⟨001⟩ zone axis.

presence of the glycolate layer, binding energies characteristic of the interstitial carbons intrinsic to carbides were not observed (S9). The interstitial C atoms were identified by chemically etching Co atoms from the surface of the particles, revealing the interstitial C atoms in the form of a carbon shell (S10).[29]

The synthesis of pure phase Co_3C and Co_2C offers a unique opportunity to characterize and identify the microscopic mechanisms leading to the emergent magnetic behavior associated with each phase. The experimental studies enabled the identification of the crystalline phases including lattice parameters and atomic coordinates for each phase that could enable theoretical investigations. Previous theoretical studies[30] on Co_2C predict that the material is non-magnetic. These studies were carried out within a density functional framework using the gradient corrected functional. As indicated above, the present experimental studies indicate that the Co_2C nanoparticles are magnetic with a substantial magnetization. Note that it is now well known that the correlation effects are important in carbides and oxides. We, therefore, carried out theoretical studies of the magnetic moment at the Co-site in Co_2C using a gradient corrected (GGA) functional as used in previous works, a GGA+U functional, and a hybrid B3LYP functional. The studies were carried out using the Vienna *ab initio* simulation package (VASP).[31] The projector-augmented wave method was used to model electron-ion interaction and the valence states of Co and C were described by [Ar] $3d^8 4s^1$ and [He] $2s^2 2p^2$ electron configurations, respectively.[32] The exchange correlation contributions were incorporated using a hybrid functional B3LYP.[33] We also attempted generalized gradient functional proposed by Perdew, Burke, and Ernzerof in a GGA+U approach with a U value of 4.0 eV to find similar results.[34] A plane wave basis with an energy cutoff of 400 eV was used and a Mokhorst-Pack scheme of $9 \times 9 \times 9$ division was used to generate the special k-points for constructing the charge density.[35] The magnetocrystalline anisotropy energy (MAE) was calculated using the contribution from spin-orbit coupling. For the Co_2C and Co_3C phases, the structures based on the x-ray diffraction were further optimized till the forces dropped below a threshold value of 0.02 eV/Å. Calculations using the GGA functional yielded a zero magnetic moment at the Co site, in agreement with previous studies. However, studies using a B3LYP functional or a GGA+U functional with a U of 4.0 eV yielded a moment of around 1.0 μ_b per Co atom, in agreement with observed magnetic phase. These findings reinforce that a proper inclusion of correlation effects is important to account for the magnetic behavior and in the remainder of the paper, we present results based on GGA+U functional. Our investigations focused on the nature of the electronic states, the magnetic moment, and the MAE associated with the Co_2C and Co_3C phases, We first carried out studies on pure β-Co, where our calculated magnetic moment of 1.86 μ_b per atom is close to the experimental moment of 1.81 μ_b. A similar calculation on α-Co yielded a moment of 1.63 μ_b, again close to the experimental value of 1.75 μ_b. For the carbide material, we calculated the total density of states as well as local density of states at the Co and C sites and these are shown in Figures 3(a) and 3(d)). The studies indicate that there is partial mixing as the C *p*-states only hybridize with Co *d*-states near the bottom of the *d*-band. The contour plots of valence charge densities show that Co_2C exhibits higher mixing between C *p* and Co *d* states than in Co_3C (Figures 3(b) and 3(e)). Consequently, both Co_2C and Co_3C are magnetic with moments of 0.99 μ_b/atom for Co_2C and 1.67 μ_b/atom for Co_3C, respectively. Furthermore, both the systems exhibit metallic character. While the mixing with C partially reduces the magnetic moment compared to the pure Co phase, it has a dramatic effect on the MAE. Bulk β-Co is a soft magnetic material (having a low coercivity, below 150 Oe) and our MAE calculations indeed indicate an easy axis along the [100] direction.[36] For the [110] and [111] directions, the results indicate a MAE per Co atom of 0.009 and 0.016 meV/atom, respectively. For the Co_2C phase, one can regard the new phase as layers of Co atoms with intervening layers of C atoms leading to an easy axis along the [001] direction and harder axis along the other directions (Figure 3(c)). Table I lists the MAE along other symmetry directions. The Co_3C phase presents a structure that could be regarded as two planes of Co atoms separated by single

Downloaded 06 Jul 2012 to 129.25.131.235. Redistribution subject to AIP license or copyright; see http://apl.aip.org/about/rights_and_permissions

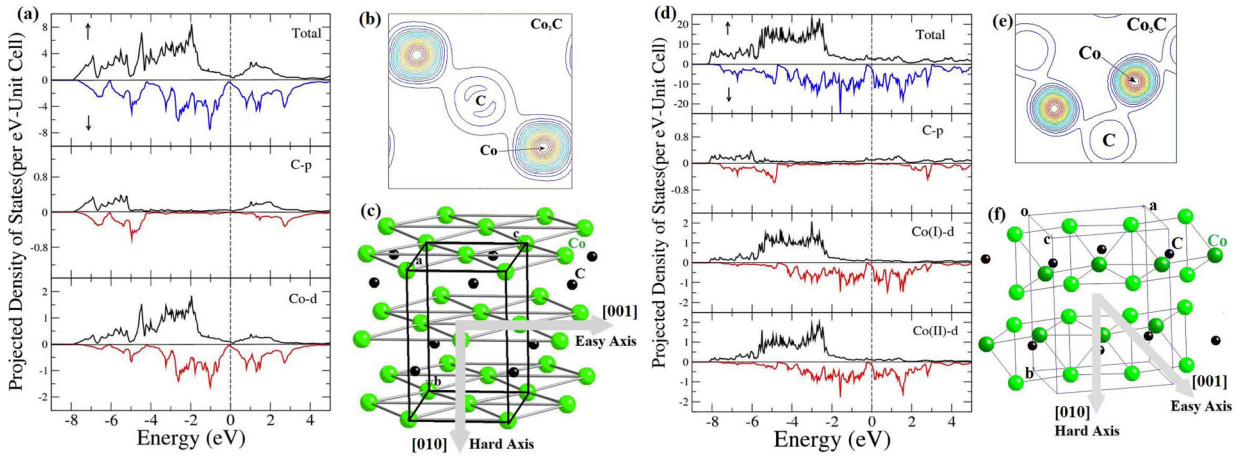

FIG. 3. Calculated total and projected densities of states of Co_2C (a) and Co_3C (d). Co(I) and Co(II) in Co_3C refer to nearest and next nearest cobalt atom from C. Majority densities are plotted as positive values; minority densities as negative values. The vertical dashed line indicates the Fermi level. Calculated valence charge densities of Co_2C and Co_3C are shown in (b) and (e), respectively. Contours are equally spaced. Calculated crystal structures with magnetically easy and hard axes are identified for Co_2C (c) and Co_3C (f).

plane of C atoms along the [010] axis (Fig. 2). This creates a [001] easy axis and the MAE increases considerable along other directions (Figure 3(f) and Table I). Thus, we believe that the addition of C, while slightly quenching the local magnetic moment, induces considerable uniaxial anisotropy, particularly for the Co_3C phase, and results in the high coercivity experimentally verified in the Co_xC nanoparticle assemblies.

The theoretical findings are in close agreement with the experimental observations. For example, single phase Co_2C was found to possess a lower coercivity (450–1200 Oe) and low magnetization (13 emu/g) while single phase Co_3C showed a higher coercivity (1.6–2.1 kOe) and high saturation magnetization (55 emu/g) (Figures 4(a) and 4(b)). However, the random particle nature of the Co_3C particles coupled with the uniaxial magnetic anisotropy of the Co_3C structure causes demagnetizing magnetostatic interactions between neighboring Co_3C grains leading to less than optimal coercivities (Figures 4(c) and 4(d)).[26,37,38] By doping in the less coercive Co_2C phase, these magnetostatic interactions between the Co_3C grains can be minimized, and exchange coupling becomes the dominant intergranular magnetic interaction (Figure 4(c)). This substantial exchange coupling in the Co_3C and Co_2C composite particles led to the highest coercivities (3.0–3.2 kOe) observed. Although, increasing the Co_2C composition to higher concentrations (>80%) causes a decoupling between the Co_3C and Co_2C phases and a bimodal coercivity distribution (Figure 4(d)). Grain size also had an effect on coercivity values for the Co_xC particles, with lower grain sizes increasing exchange coupling and enhancing coercivity.

TABLE I. MAE of bulk Co_2C and Co_3C in units of meV per formula obtained by GGA+U (U = 4 eV) calculations. The zero energy is set as the reference and the corresponding direction is the easy axis.

	[100]	[010]	[001]	[110]	[111]
Co_2C	0.156	0.203	0	0.180	0.120
Co_3C	0.178	0.206	0	0.191	0.128

The common metric for permanent magnets is energy product, or BH_{max}, which can be simplistically viewed as the product of magnetization and resistance to demagnetize (coercivity). In this study, we have experimentally and theoretically identified Co_3C to have both a higher magnetization and coercivity when compared to Co_2C. Theoretical studies indicate that the mixing between the Co *d*- and C *p*-states, while slightly reducing the pure Co moment, does enhance the magnetic anisotropy of the carbide phases with a higher value for the Co_3C. The actual nano-composite consists of a mixture of Co_3C and Co_2C nanoparticles. The resulting properties are, therefore, governed by those of the pure phases as well as by the nature of the interface and the exchange coupling between the nanoparticles.

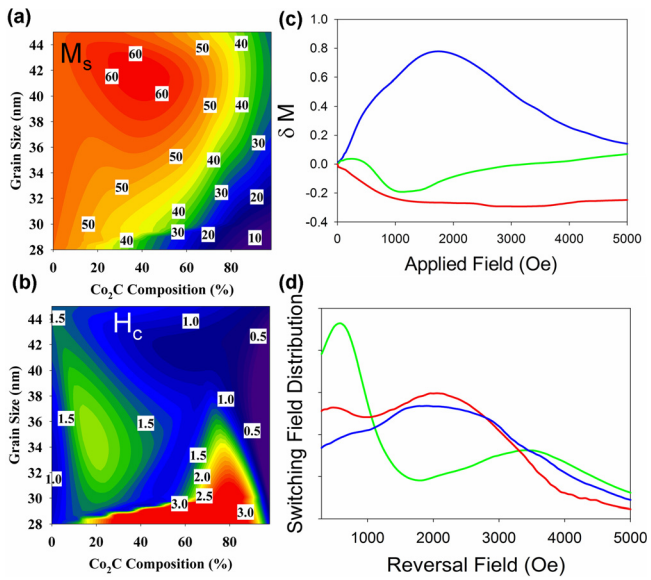

FIG. 4. Contour plots showing the effect of phase composition and grain size on (a) saturation magnetization in emu/g and (b) coercivity in kOe. (c) Henkel plots and (d) reversal field distribution for pure phase Co_3C (red), Co_3C rich composites (blue), and Co_2C rich composites (green). Henkel plots are derived from the isothermal remanent magnetization (IRM) and direct current demagnetization (DCD) values (S11) using the equation: $\delta M = M_{DCD} - (1 - 2M_{IRM})$, see Ref. 39.

Downloaded 06 Jul 2012 to 129.25.131.235. Redistribution subject to AIP license or copyright; see http://apl.aip.org/about/rights_and_permissions

Synthetically, we are able to manipulate the Co_3C and Co_2C phase composition through intricate control of $[OH^-]$ and reaction temperature when using the polyol process with TEG as the solvent. The present study suggests that the addition of C is critical to controlling the anisotropy and also suggests that even higher energy products could be attained via the proper selection of transition metal, non-metal element, and shape and morphology. The ability to control these parameters synthetically opens a path to minimizing rare earth dependency by creating a class of permanent magnets that rival that of the current state of the art technologies.[40]

K.J.C, D.H, E.E.C, and Z.H acknowledge support from NSF-MRI Grants #CHE0820945 and #CHE0922582. They also acknowledge the support from the NCC facilities at VCU. D.H. and E.E.C. acknowledge support from the U.S. Department of Energy (ARPA-E). S.N.K. and M.Q. acknowledge support from Air Force Office of Scientific Research under AFOSR Award No. FA9550-09-1-0371 for theoretical studies. S.R.S. and M.L.T. would like to acknowledge the use of Drexel University's Centralized Research Facilities.

[1]O. Gutfleisch, M. A. Willard, E. Bruck, C. H. Chen, S. G. Sankar, and J. P. Liu, Adv. Mater. **23**, 821 (2010).
[2]S. Sugimoto, J. Phys. D: Appl. Phys. **44**, 11 (2011).
[3]H. W. Zhang, G. Long, D. Li, R. Sabirianov, and H. Zeng, Chem. Mater. **23**, 3769 (2011).
[4]V. G. Harris, Y. Chen, A. Yang, S. Yoon, Z. Chen, A. L. Geiler, J. Gao, C. N. Chinnasamy, L. H. Lewis, C. Vittoria, E. E. Carpenter, K. J. Carroll, R. Goswami, M. A. Willard, L. Kurihara, M. Gjoka, and O. Kalogirou, J. Phys. D: Appl. Phys. **43**, 7 (2010).
[5]M. E. McHenry, J. M. MacLaren, and D. P. Clougherty, J. Appl. Phys. **70**, 5932 (1991).
[6]P. R. Ohodnicki, V. Keylin, H. K. McWilliams, D. E. Laughlin, and M. E. McHenry, J. Appl. Phys. **103**, 07E740 (2008).
[7]M. E. McHenry, S. A. Majetich, J. O. Artman, M. DeGraef, and S. W. Staley, Phys. Rev. B **49**, 11358 (1994).
[8]Y. Zhang, G. S. Chaubey, C. Rong, Y. Ding, N. Poudyal, P.-C. Tsai, Q. Zhang, and J. P. Liu, J. Magn. Magn. Mater. **323**, 1495 (2011).
[9]K. J. Carroll, J. U. Reveles, M. D. Shultz, S. N. Khanna, and E. E. Carpenter, J. Phys. Chem. C **115**, 2656 (2010).
[10]D. Ung, Y. Soumare, N. Chakroune, G. Viau, M. J. Vaulay, V. Richard, and F. Fievet, Chem. Mater. **19**, 2084 (2007).
[11]D. Ung, G. Viau, C. Ricolleau, F. Warmont, P. Gredin, and F. F. Fievet, Adv. Mater. **17**, 338 (2005).
[12]N. E. Tsakoumis, M. Ronning, O. Borg, E. Rytter, and A. Holmen, Catal. Today **154**, 162 (2010).
[13]J. Cheng, P. Hu, P. Ellis, S. French, G. Kelly, and C. M. Lok, J. Phys. Chem. C **114**, 1085 (2010).
[14]S. Stolbov, S. Y. Hong, A. Kara, and T. S. Rahman, Phys. Rev. B **72**, 155423 (2005).
[15]J. Lahiri, T. Miller, L. Adamska, I. I. Oleynik, and M. Batzill, Nano Lett. **11**, 518 (2011).
[16]J. P. Huo, H. H. Song, X. H. Chen, S. Q. Zhao, and C. M. Xu, Mater. Chem. Phys. **101**, 221 (2007).
[17]A. Wiltner and C. Linsmeier, Phys. Status Solidi A **201**, 881 (2004).
[18]J. J. C. Geerlings, M. C. Zonnevylle, and C. P. M. de Groot, Surf. Sci. **241**, 315 (1991).
[19]J. Xiong, Y. Ding, T. Wang, L. Yan, W. Chen, H. Zhu, and Y. Lu, Catal. Lett. **102**, 265 (2005).
[20]M. Kollar, A. De Stefanis, H. E. Solt, M. R. Mihalyi, J. Valyon, and A. A. G. Tomlinson, J. Mol. Catal. A **333**, 37 (2010).
[21]K. F. Tan, J. Xu, J. Chang, A. Borgna, and M. Saeys, J. Catal. **274**, 121 (2010).
[22]R. Beck, U. Florke, and H. F. Klein, Inorg. Chem. **48**, 1416 (2009).
[23]N. Chakroune, G. Viau, C. Ricolleau, F. Fievet-Vincent, and F. Fievet, J. Mater. Chem. **13**, 312 (2003).
[24]C. N. Chinnasamy, B. Jeyadevan, K. Shinoda, K. Tohji, A. Narayanasamy, K. Sato, and S. Hisano, J. Appl. Phys. **97**, 3 (2005).
[25]G. Viau, C. Garcia, T. Maurer, G. Chaboussant, F. Ott, Y. Soumare, and J. Y. Piquemal, Phys. Status Solidi A **206**, 663 (2009).
[26]Y. Soumare, C. Garcia, T. Maurer, G. Chaboussant, F. Ott, F. Fievet, J. Y. Piquemal, and G. Viau, Adv. Funct. Mater. **19**, 1971 (2009).
[27]I. G. Wood, L. Vocadlo, K. S. Knight, D. P. Dobson, W. G. Marshall, G. D. Price, and J. Brodholt, J. Appl. Cryst. **37**, 82 (2004).
[28]I. R. Shein, N. I. Medvedeva, and A. L. Ivanovskii, Phys. B: Condens. Matter **371**, 126 (2006).
[29]Z. L. Schaefer, M. L. Gross, M. A. Hickner, and R. E. Schaak, Angew. Chem., Int. Ed. **49**, 7045 (2010).
[30]Y.-H. Zhao, H.-Y. Su, K. Sun, J. Liu, and W.-X. Li, Surf. Sci. **606**, 598 (2012).
[31]G. Kresse and J. Furthmuller, Phys. Rev. B **54**, 11169 (1996); G. Kresse and J. Hafner, J. Phys.: Condens. Matter **6**, 8245 (1994).
[32]G. Kresse and D. Joubert, Phys. Rev. B **59**, 1758 (1999).
[33]A. D. Becke, J. Chem. Phys. **98**, 1372 (1993).
[34]S. L. Dudarev, G. A. Botton, S. Y. Savrasov, C. J. Humphreys, and A. P. Sutton, Phys. Rev. B **57**, 1505 (1998); J. P. Perdew, K. Burke, and M. Ernzerhof, Phys. Rev. Lett. **77**, 3865 (1996).
[35]H. J. Monkhorst and J. D. Pack, Phys. Rev. B **13**, 5188 (1976).
[36]G. Y. Guo, D. J. Roberts, and G. A. Gehring, Phys. Rev. B **59**, 14466 (1999).
[37]Y. Sun and Y. F. Wan, J. Alloys Compd. **509**, 6139 (2011).
[38]T. Maurer, F. Zighem, W. Fang, F. Ott, G. Chaboussant, Y. Soumare, K. A. Atmane, J.-Y. Piquemal, and G. Viau, J. Appl. Phys. **110**, 123924 (2011).
[39]E. P. Wohlfarth, J. Appl. Phys. **29**, 595 (1958).
[40]F. Ott, T. Maurer, G. Chaboussant, Y. Soumare, J. Y. Piquemal, and G. Viau, J. Appl. Phys. **105**, 1 (2009).
[41]See EPAPS supplementary material at http://dx.doi.org/10.1063/1.4733321 for detailed description of experimental and characterization procedures and supporting data.

Downloaded 06 Jul 2012 to 129.25.131.235. Redistribution subject to AIP license or copyright; see http://apl.aip.org/about/rights_and_permissions